Contrib. Astron. Obs. Skalnaté Pleso **35**, 180 – 198, (2005)

Bimodal differential rotation of the solar corona

O.G. Badalyan[1] **and J. Sýkora**[2]

[1] *Institute of Terrestrial Magnetism, Ionosphere and Radio Wave Propagation, 142190 Troitsk, Russia*

[2] *Astronomical Institute of the Slovak Academy of Sciences 059 60 Tatranská Lomnica, The Slovak Republic*

Received: June 10, 2005; Accepted: September 21, 2005

Abstract. Spectral Variation Analysis (SVAN) was applied to our own database of Coronal Green Line Brightness (CGLB) covering almost six solar cycles (1939-2001) to investigate differential rotation of the solar corona. Detailed knowledge of solar rotation seems to be crucial for a better understanding of the basic mechanisms of solar activity generation. The following principal results were obtained: (a) The synodic period of coronal rotation increases from 27 days at the equator to about 29 days at the latitudes of $\pm 40^\circ$, displaying the less pronounced differentiality than the photospheric phenomena do. (b) Above $\sim \pm 45^\circ$ differentiality greatly diminishes and the rotation displays actually rigid character (with the period of about 29.5 days) up to polar regions. (c) The total corona rotation may be expressed as a sum of two modes, the faster one with period of 27 days (slightly increasing towards the higher latitudes), and the slow one with the period of about 30.5 days; the relative contribution of these modes to the total rotation rate is estimated in dependence on latitude. A short comment on relation of our findings with the latest achievements of helioseismology is given.

Key words: solar corona – coronal green line brightness – differential rotation – two modes of rotation – helioseismology

1. Introduction

Discovery of the solar rotation dates, in fact, back to the first telescopic observations of sunspots at the beginning of the seventieth century and the phenomenon was continuously studied due to recognizing its crucial importance for any theory describing observed evolution, variabilities and periodicities in the solar activity. Though a huge number of observational facts were recorded in the past, still new details are being observed and old puzzles, such as the origin of the differential rotation itself, remain unsolved. Except for that and due to that, any quantitative theory is missing to tie up together the large-scale convection, differential rotation and meridional flows on the Sun. Thus, additional analysis of the new data and accessible databases could be still helpful.

The solar rotation can be measured from observations of the angular displacements of semipermanent features in the solar atmosphere as, e.g., recurrent spots, all spots, faculae, flocculi, dark filaments, low-level magnetic features, Ca K network, bright points, coronal holes, etc. (using the so-called method of tracers), or from spectroscopic observations (measuring the Doppler shifts of, namely, photospheric spectral lines). Correlations of full disk magnetograms provide also a good way to determine the solar rotation. Each method yields somewhat different latitudinal dependence though most tracers show the same rotation rate at the equator.

Although the above methods are in principle straightforward, their accuracy is limited by a number of random and systematic errors and no preference to one of the methods may be unambiguously attributed (see, e.g., Schröter, 1985 and Snodgrass, 1992). As for the tracer method, inaccuracy follows mainly from the proper and often unpredictable surface motions of the various tracers during their evolution. The method using Doppler shifts is affected by several systematic troublesome determined errors, as well. Among them are stray light of instrumental and Earth-atmospheric origins, spectrum affected by the local solar velocities at the observed positions. In addition, it should be kept in mind that the spectroscopic measurements always yield the line of sight velocities only.

Nowadays, sophisticated helioseismic measurements provide a reliable picture of the Sun's angular velocity as a function of both the depth and the latitude. Therefore, helioseismology has the potential to give a nearly complete picture of the rotation throughout the solar interior, thus offering very powerful new tool (instrument) constraints for modelling the way how convection, rotation and magnetic field interact to produce differential rotation and the solar dynamo.

It is far beyond scope of this paper to summarize historical and scientific achievements of the extended topic on solar rotation. Nevertheless, at least, the latest topical reviews and monographs dealing with behavior of solar rotation as derived from various features of solar activity in different layers of the Sun's atmosphere should be mentioned (Schröter, 1985; Bogart, 1987; Rüdiger, 1989; Librecht and Morrow, 1991; Snodgrass, 1992; Schrijver and Zwaan, 2000; Foukal, 2004; Stix, 2004). The basic observational facts (results) may be enumerated as follows:

(a) The Sun doesn't rotate like a solid body but its angular velocity varies with latitude and depth. Low latitudes rotate at a faster angular rate than do the higher latitudes. This effect is called differential rotation. Newton and Nunn (1951) found no measurable variations of solar rotation (the recurrent groups of spots recorded over 1878-1944 period were investigated) either with alternate 11-year cycles or within the cycle itself and their classical law of rotation $\omega = 14^{\circ}.38 - 2.77 sin^2\phi$ is still respected as "an etalon".

(b) Generally, the rotation rate decreases as the size of a phenomenon or "active" region increases (Howard, 1990). It is tempting to interpret this result in

terms of rooting depths, assuming the larger regions are more deeply rooted. A gradual decrease in rotation with depth is consistent with recent results in helioseismology.
(c) There is an 11-year pattern of rotation rate changes related to the activity cycle with increase at solar minimum and perhaps also at solar maximum. Other phases of the cycle are characterized by a reduced rotation rate. No uncontroverted evidence for longer-term, or secular, changes were reported.

The pattern of the coronal green line brightness (CGLB), representing emission in the Fe XIV 530.3 nm forbidden spectral line, has been used as a tracer of the Sun's (coronal) rotation in numerous past investigations (Trellis, 1957; Sýkora 1971, 1980, 1994; Antonucci and Svalgaard, 1974; Letfus and Sýkora 1982a, 1982b; Sime et al, 1989; Rybák 1994, 2001; Badalyan and Sýkora 2005). All the authors derived benefit from quantitative CGLB data measurable over the whole range of solar latitudes and covering several solar cycles (the CGLB data are now available since 1939). The principal effects detected (found) in the past are (a) a less pronounced differentiation of coronal rotation than that of the most solar surface phenomena and, (b) a quasi-rigid rotation above $40^\circ - 50^\circ$ of solar latitude. It actually means that two modes (fast and slow) could be present in the rotation law of the solar corona. It is expectable that a mutual prevalence of one or another mode is cycle-phase-dependent (Mouradian et al., 2002). In the present paper most of our previous results on coronal rotation are developed and up-to-dated.

It should be perhaps mentioned that similar enough behavior to the CGLB rotation was found by analysis of the white-light and radio corona (Hansen et al., 1969; Fisher and Sime, 1984; Parker, 1986; Mouradian et al., 2002) and for the large-scale photospheric solar magnetic field (Stenflo, 1989). Moreover, Sheeley at al. (1987), Wang et al. (1989) and Wang and Sheeley (1993) have developed a theoretical approach to the bimodal behavior of rotation rates in the solar atmosphere. They demonstrated that this behavior can be explained purely by surface flows (e.g., differential shear, meridional flows), and the eruption and diffusion of concentrated magnetic flux. Modelling the rotational modulation of the Sun as a star (Lanza et al., 2003) and differential rotation related to meridional circulation near the boundaries of the solar convective zone (Kichatinov, 2004) complete the latest attempts to provide theoretical understandings of a variety of features observed in rotation and differential rotation of the Sun's body.

Intensity of the brightest emission line Fe XIV 530.3 nm of the optical solar corona is, indeed, a very informative index of solar activity. Nowadays, quite a long set of systematic patrol measurements of the CGLB is available, covering almost the last six solar activity cycles. A specific advantage of the CGLB index results from its almost simultaneous registration over the entire corona. Consequently, the CGLB index provides a homogeneous numerical field of data allowing to study different characteristics of coronal plasma by the unified pole-to-pole measurements.

Let us give a basic characterization of our CGLB database (for a short historical background and more details on observations of the Fe XIV 530.3 nm coronal emission line intensity see, e.g., Storini and Sýkora, 1997 and Badalyan et al., 2001). The patrol coronagraphic measurements, regularly (daily) carried out by a small world–wide network of high-altitude observatories, were synthesized to create photometrically homogeneous database of the Fe XIV 530.3 nm coronal emission line intensities (data for about 15% of individual days not covered by observations were interpolated). The measurements of different observatories were reduced to a common photometric scale and to the height of $60''$ above the solar limb. Thus, the initial database consists of measurements made with the temporal resolution of one day ($\sim 13^\circ$ in the solar latitude) and with the resolution of 5° in position angle.

Originally, the measurements are available from both the east and west solar limbs. From these a central meridian (CM) data were derived as an average of intensities measured 7 days before and 7 days later, i.e. as an average of values when the proper meridian passed the E and W limbs, respectively. At the same time, the original position angles were transformed to the solar latitudes. Subsequently, namely the CM data were used to construct all the figures and maps in this contribution. As a result, our CGLB database covers the 1939-2001 period. The original way of reduction of the data of different observatories was described in Sýkora (1971a).

In our opinion, the present CGLB database represents now the second longest set of data (after the sunspots) among synoptic indices of solar activity. Naturally, measurements of the CGLB obtained at individual coronal observatories were frequently spatially and temporarily analyzed in the past from many points of view. Even if there is no space here to summarize previous findings of all the authors still, the classical investigations of Trellis (1957), Waldmeier (1951, 1971) and Gnevyshev (1967, 1977) should be, at least, enumerated. Our latest papers describing a number of aspects in the large-scale and long-term distributions of coronal activity derived from analysis of the photometrically homogenized database could be also mentioned (Badalyan et al., 2004, 2005; Sýkora and Rybák 2005).

In this study, we examine the rotational characteristics of the corona as inferred from the Fe XIV 530.3 nm measurements. We restrict ourselves to description of the results on rotation and differential rotation obtained from the long-term (1939-2001) and large-scale (increments of 5° and 13° in the heliographic latitude and longitude, respectively) analysis of the Fe XIV 530.3 nm coronal green line brightness. We stress a bimodal character of the coronal rotation and its mean characteristics. Relations of our results to the theory of solar dynamo and interior rotation of the Sun revealed by recent helioseismic measurements are underlined, as well.

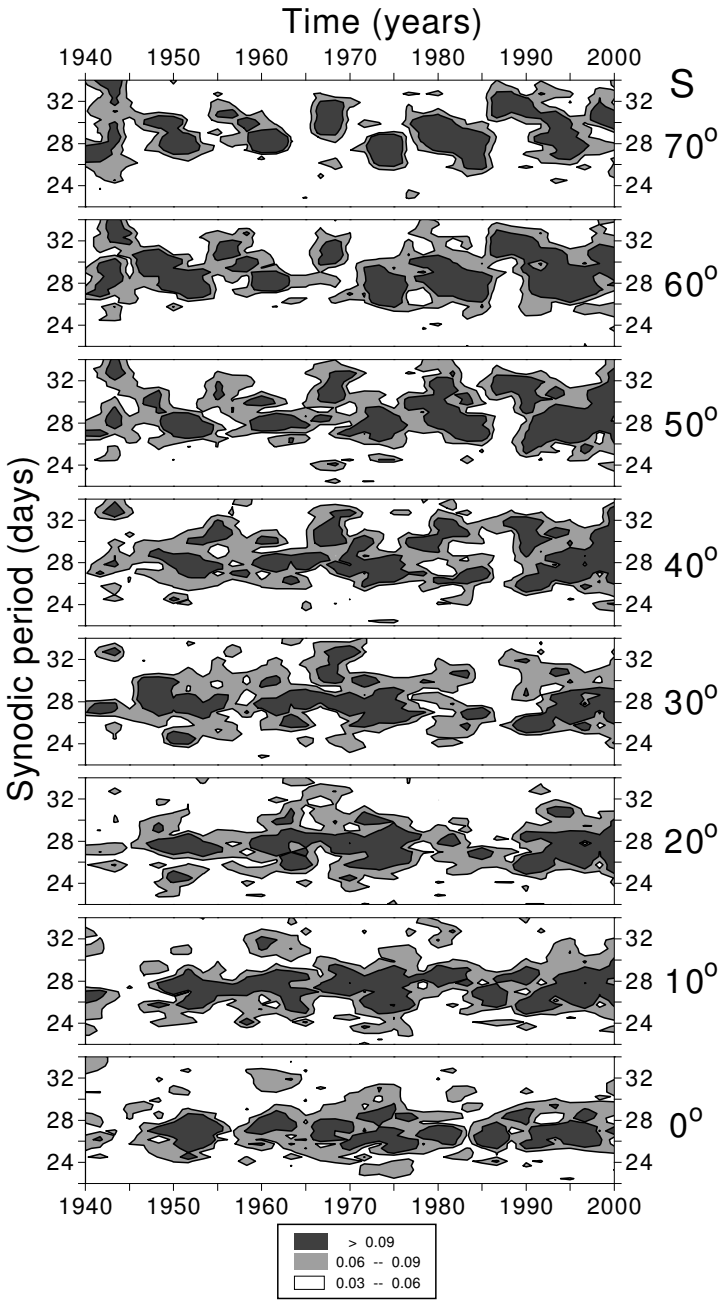

Figure 1. Examples of the SVAN diagrams for eight latitudes of the southern (S) solar hemisphere. The dark shadowing indicates the periods with the highest amplitudes and the white area denotes the periods with the lowest amplitudes.

2. Differential rotation of the solar corona

We have used the so-called Spectral Variation Analysis (SVAN) to investigate time-latitude dependence of coronal rotation. The SVAN, in fact, represents consecutive Fourier analyses in a sliding window of a certain time length. Over the chosen window the Fourier analysis is applied to the daily CGLB data. Initial data set is expanded in terms of the harmonic functions each of them having its own amplitude (power) in accordance with its contribution to the initial data. This makes it possible to extract from a number of harmonic functions that one the period of which is the closest to a "quasi-period" of the initial distribution. Then this window is shifted for a certain time interval and the whole procedure is repeated. Understandably, as a result, we obtain the recurrence periods of coronal brightness. However, all the tracer's methods are looked for, namely, the recurrence periods of any studied index. An assumption on agreement of the recurrence period with the period of rotation is possible if all the periodic modes of temporal variations of the index in question have frequencies distant from and incoherent with the frequencies (periods) of rotation.

Subsequently, the values obtained from the whole set of Fourier analyses were assembled and the final map of amplitudes in time-period coordinates (so-called SVAN diagram) was constructed for each solar latitude. In this work a 6-year window and an 81-day step of sliding were used providing 258 windows through the whole database. Within each window a normalization by division of each number by 2σ was done (σ represents the mean square deviation). During calculations, we restricted ourselves to the amplitudes within the period range of $21.9 - 36.5$ days.

It should be noted that similarly to that in the standard Fourier analysis also here the increment in frequency is constant. Therefore, the values of the interval between the periods following from the length of the expansion window are not constant but gradually increase with a number of harmonics. A possible number of all harmonics in the expansion is equal to the number of points N in the chosen expansion window, i.e., the period of the window length corresponds to the first harmonics and the step between the data (in our case it is one day) corresponds to the last harmonics. In the present work our own original program of the SVAN was used. It differs from those commonly described in the literature (see, e.g., Dzewonski et al., 1969) by the fact that in each expansion window a division by 2σ (where σ is the mean square deviation) is performed. Consequently, the sum of the squares of amplitudes of all the possible periods is equal to one in each window.

The SVAN was performed for each latitude separately, therefore, 35 SVAN diagrams were obtained within $\pm 85^\circ$ of latitude. Considering an understandable increasing error level of the CGLB measurements at the highest latitudes, connected basically with lengthening of the effective longitudinal interval to which the registered integral line intensity relates considerably increases at those latitudes, we have limited our present investigation to $\pm 75^\circ$ of latitude only.

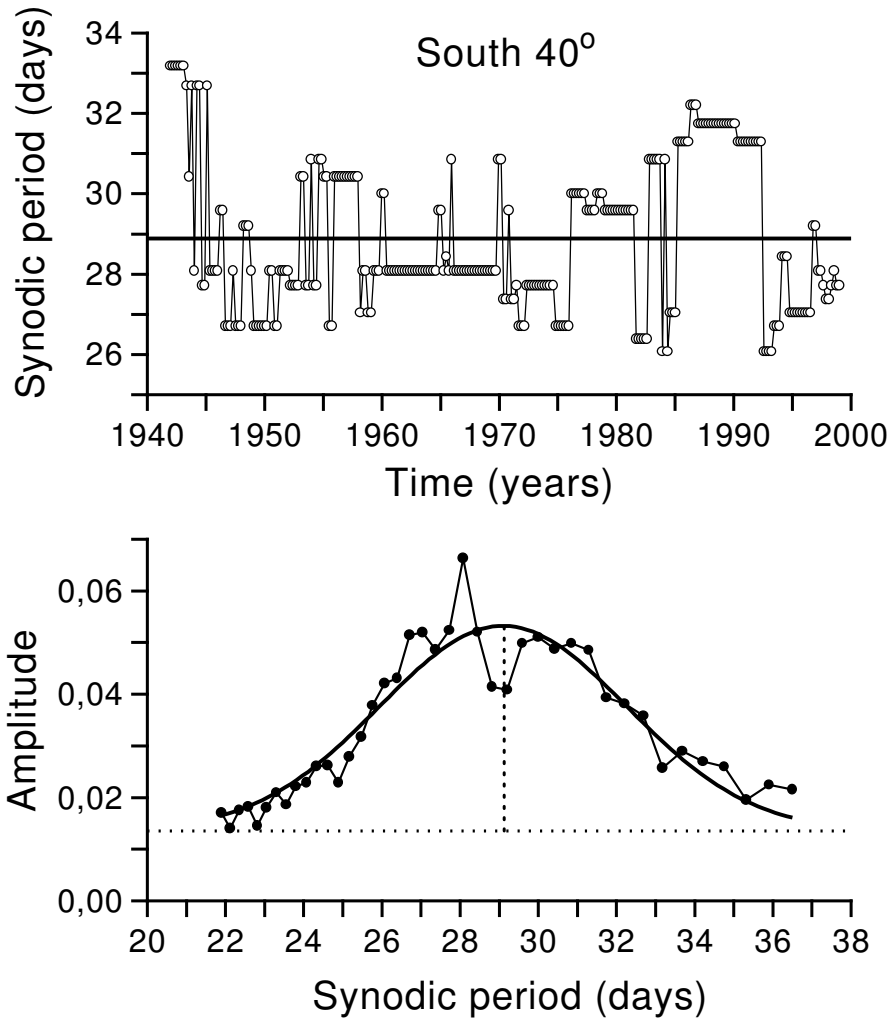

Figure 2. An example of determination of the period of coronal rotation by the method of maximal amplitudes for 40° of the southern hemisphere (upper panel). Individual open circles correspond to the windows. The full horizontal line indicates the mean of all these periods. The lower panel shows an example of "a mean spectrum" approximation (full circles – 41 points from all the included periods in our calculations), by a gaussian curve. Maximum of the curve is indicated by the dotted lines while the horizontal dotted line represents the baseline offset (see the text).

Fig. 1 shows eight examples of the SVAN diagrams for different latitudes of the southern (S) solar hemisphere. Dark regions indicate the periods with the highest amplitudes while white areas denote the periods with the lowest amplitudes. The legend below indicates three displayed intervals of the amplitudes of periods. We remind again that the sum of squares of all the possible amplitudes in each expansion window is equal to one by our definition. Fig. 1 also demonstrates how a general pattern of the charts and position of the bands of highest amplitudes on them varies in dependence on the solar latitude. Evidently, moving towards the higher latitudes the belt of the highest amplitudes shifts to the longer periods (along the Y axis) and becomes broader. This means that at the higher latitudes still longer periods become more prevailing within the expansion. A value of the period approximately corresponding to the middle of the belt with the highest amplitudes in each period-time map is considered to be the period of rotation at the given latitude. Therefore, shifting the amplitude belt in Fig. 1 to the higher periods implies a certain retardation of coronal rotation rate with increasing latitude. Below, we offer some interpretation of the mentioned amplitude belt broadening.

We have determined the period of coronal rotation as follows. In each of the 258 SVAN windows the period with the maximal amplitude was sought out. These periods represent some chronological sequentiality. Then, the mean value of them was accepted as the period of coronal rotation at the given latitude. In what follows, this method of determination the period of coronal rotation will be called as "the method of maximal amplitudes". An example of such determination of the rotation period is depicted in Fig. 2 (upper panel) where the open circles indicate 258 periods found in the sliding SVAN window and the horizontal line represents a mean value of the rotation period for the corresponding latitude (in this case approximately 28.9 days for south 40°). Subsequently, from the whole set of the periods found for different solar latitudes a final dependence of coronal rotation on latitude may be derived.

Another possible way how to determine the rotation rate of the corona may be based on fitting by the gaussian curve the whole set of amplitudes of all the 41 periods found by SVAN in all the 258 successively sliding windows at a given latitude. An example of such a procedure is shown in the lower panel of Fig. 2. To construct this type of graph, for each period a mean value of its amplitude was found in all 258 windows (full circles), i.e., a certain "averaged spectrum" was derived. Then these points were fitted by a gaussian curve. In fact, this procedure represents a drawing the gaussian curve by fitting distribution of all the 258×41 points. The vertical dotted line indicates position of the gaussian curve maximum (in this particular case it is 29.1 days). This period may well be considered as the period of coronal rotation at a given latitude (in this case at 40° south). The aggregate of such determinations for all the solar latitudes allows us to draw a dependence of the synodic period of coronal rotation on the Sun's latitude as well.

All the determinations of the periods of coronal rotation by the two above

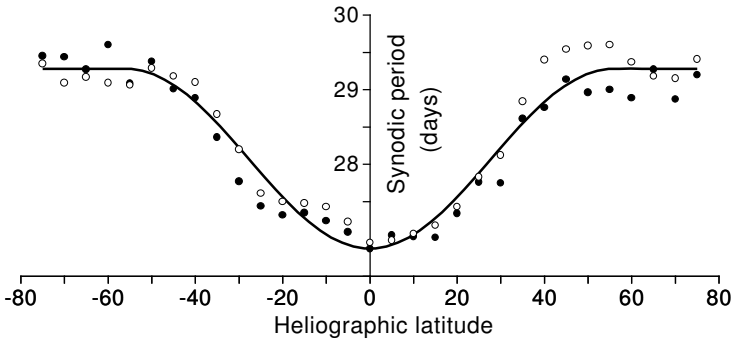

Figure 3. Variation of the coronal rotation with the heliographic latitude. By the full and open circles the results obtained by the method of maximal amplitudes and by the fitting with gaussian curve are shown, respectively.

described methods are compiled in Fig. 3. Here, the full circles stand for the periods obtained by the method of maximal amplitudes while the open circles signify the periods derived by fitting the gaussian curves. One can see, firstly, that these two methods provide the results not differing substantially from each other and, secondly, that the periods found for the northern and southern hemispheres are practically the same. The mean, symmetrical to the ordinate axis, curve was obtained by the following manner. In the next, all the points related to the southern hemisphere were mirrored from the left half of the figure to its right part. Then, all the points (four values for each latitude) were fitted by a curve and this was, subsequently, symmetrically re-drawn onto the left part of Fig. 3. By this way a mean curve of coronal rotation, showing dependence of the synodic period on solar latitude, was obtained using both the maximal amplitudes method and the gaussian curve fitting.

Fig. 3 shows that within the limits of accuracy the northern and southern hemispheres exhibit identical dependence. The periods are close to 27 days at low latitudes, then, above 15° the period increases (i.e., the rotation rate decreases) and slightly exceed 29 days at about 45°. Above $45° - 50°$ the coronal rotation rate remains more or less constant.

3. Two modes of coronal rotation

In the preceding Section we have brought some general characteristics of coronal rotation. However, a number of observational facts give evidence that the coronal rotation is much more complex. In the present Section one of possible interpretations of the found space- and time-dependence of the rotational periods is treated.

A detailed investigation of the whole set of the period-time maps has revealed that for the latitudes above 20° the belt of the highest amplitudes, together with the broadening at higher latitudes, seems to split into two secondary belts. This evokes an idea to explain the observed coronal rotation by a superposition of two modes of rotation considering different input of them into the general dependence of rotation on latitude. Such a possibility arises also from Fig. 3. One may imagine that at low latitudes a fast mode and at high latitudes a slow mode are dominating, respectively. At the same time, at middle latitudes some "mixture" of these two modes could be effective. In addition to, the maps in Fig. 1 show that from time to time one or another mode is dominant at a given latitude (see relocation of the darkest areas from the longer to the shorter periods, and vice versa). This is also seen in the upper panel of Fig. 2 where at two adjacent open circles (corresponding to two adjacent SVAN windows) the period may change for 4-5 days. Comparison of Fig. 2 with Fig. 1 indicates that such changes of rotation period are most likely real and may be interpreted as a transition to domination of alternating mode at a given latitude.

Let's discuss in more detail the broadening of the belt of highest amplitudes seen on the charts as presented in Fig. 1 Results of calculations obtained by using the SVAN indicate that both the dispersion of points at the upper panel of Fig. 2 and the width of the gaussian curve at the lower part of this figure increase with the solar latitude (in agreement with the broadening of the highest amplitudes belt in Fig. 1. This is demonstrated in Fig. 4. The upper panel of this figure shows latitudinal dependence of parameter σ (mean square deviation of points in the graphs of type as in the upper panel of Fig. 2) from their mean value at a given latitude (the horizontal line in Fig.2). The σ quantity characterizes by a certain way the dispersion of the points obtained by the method of maximal amplitudes. In other words, it characterizes deviation of the period with the maximal amplitude in a particular expansion window of the SVAN from a mean value of such periods in all 258 windows at a given latitude. In case that the dispersion of these values would characterize a random error in determination of the periods only, resulting from observational errors, their treatment and the method of analysis, then, distribution of the periods obtained in the 258 windows should be close to the law of normal distribution of random values. However, as the upper panel of Fig. 2 and other similar graphs show, the deviations of the points differ from the normal law. If to describe these deviations in terms of two modes of rotation then the broadening of the belt of the highest amplitudes can be interpreted as a latitudinal variation of contribution of each of these modes to a general averaged rotation rate. In this case, the upper panel of Fig. 4 indicates that at lower latitudes the fast mode (lower periods) dominates, the slow mode is practically absent and the belt of the highest amplitudes is relatively narrow. At the middle latitudes the contribution of both the modes becomes comparable and the curve in Fig. 4 reaches its local maximum. At the higher latitudes the slow mode becomes to dominate, the width of the amplitude belt being again somewhat lesser. A certain increase in dispersion of points at the latitudes of

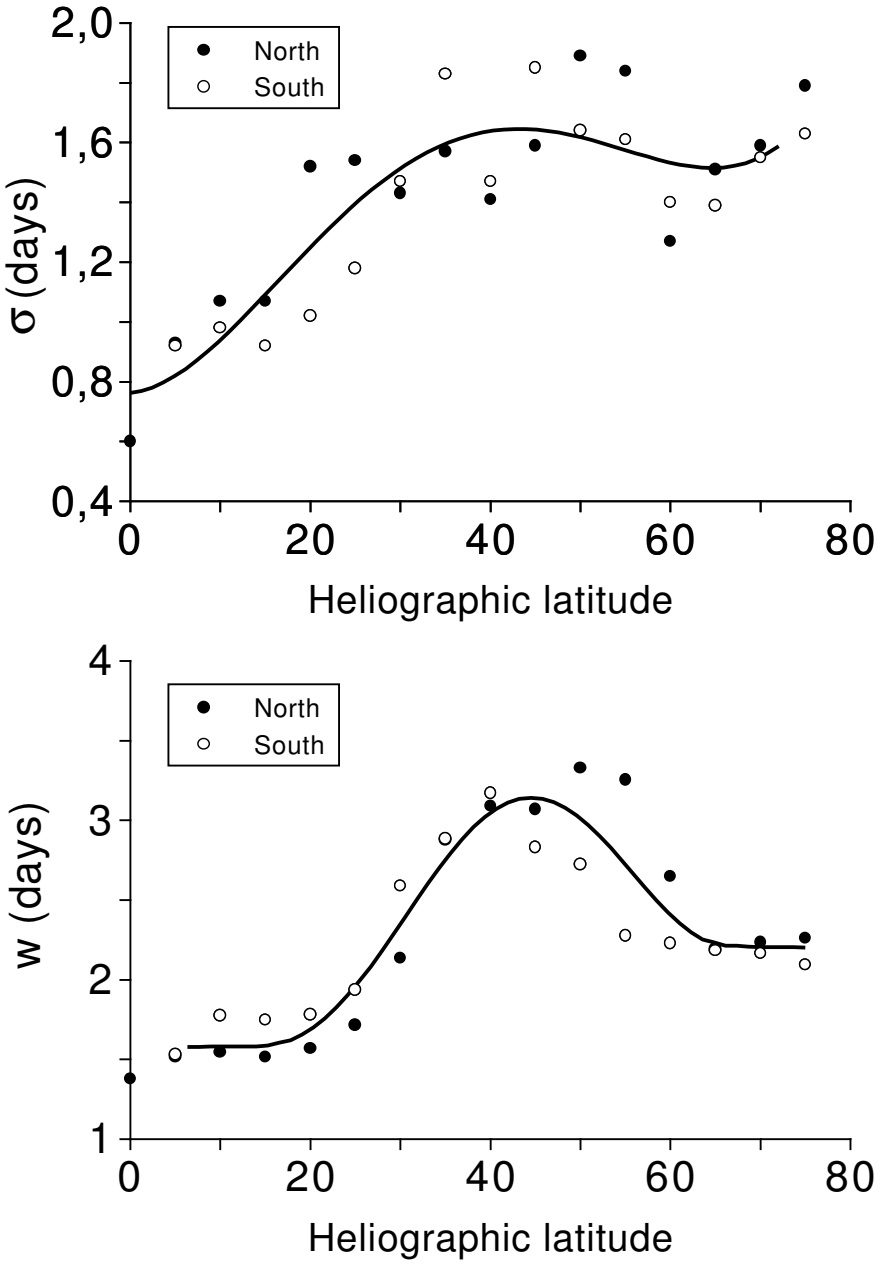

Figure 4. The upper panel shows the mean square deviations from their mean value on the graphs of type as in the upper panel of Fig. 2 and the lower panel presents the widths of the gaussian curves (see the text).

70° and more on the graphs as that in the upper panel of Fig. 2, apparently, already reflects an increasing uncertainty in determination of the periods by the method of maximal amplitudes.

At the lower panel of Fig. 4 the variations of the gaussian curve width in dependence on latitude are presented. We bring on this graph a parameter w extracted from the Gauss function G written in the form:

$$G(y) = \frac{A}{w\sqrt{2\pi}}\ exp(-\frac{(x-x_0)^2}{2w^2}) + y_0. \quad (1)$$

Here y_0 is baseline offset the (horizontal dotted line in the lower panel of Fig. 2); x_0 denotes the peak of the gaussian curve (above the horizontal dotted line) and A represents an area under the peak. Parameter w has the same meaning as σ parameter in the law of the normal distribution of random values. The $2w$ quantity is close to the width of the peak at half of the curve height (more precisely, it is less of it by about $\sqrt{2\ln 2} \approx 1.18$). Understandably, the width of the gaussian curve also reflects widening of the belts of the pronounced periods, having the large amplitudes. Because, as it was noted above, our gaussian curve represents amplitudes of all 258×41 periods (unlike to only selected periods with highest amplitudes, such as those in the upper panel of Fig. 2), here influence of the random deviations is more relevant and w is closer to σ in the normal distribution law than the mean square deviation, brought in the upper panel of Fig. 4.

As it follows from the lower panel of Fig. 4, here the curve reaches the maximum also at the middle latitudes (approximately at the same latitudes as in the upper panel of this figure) what can be interpreted as an increase of the slow mode contribution with the increasing latitude. At the high latitudes the contribution of the fast mode is lesser and the width of the gaussian curve decreases as well. The values w alone are about two times higher than the σ values in the upper panel of Fig. 4. Evidently, this is connected with the fact that the upper panel gives dispersion of the selected periods at a given latitude while the lower panel describes dispersion of all the periods.

Thus, we will consider a possibility of representation of the observed periods of coronal rotation as a result of a mutual synthesis of two modes. It is clear that a general task to decompose the coronal rotation into two modes is undefined and ambiguous. To realize such a decomposition some additional conditions are necessary to be introduced. These conditions can be introduced by a different way being guided by some experimental and/or theoretical conceptions.

Considering the structuralism of the whole set of the period-time maps (similar to those in Fig. 1) we adopted such a condition. In these maps (and also in the graphs as presented in the upper panel of Fig. 2) one can see that the splitting of the belt of the highest amplitudes occurs approximately at a level of the 29-day period. Therefore, one may assume that the periods of rotation lower than 29 days are related to the fast mode and those exceeding 29 days to the

slow mode. In other words, the fast mode manifests periods of rotation around 27.5 days and the slow mode concentrates around a period of 30-31 days.

Therefore, to find out two modes of coronal rotation we assumed that the value of 29 days separates the periods related to the fast mode from those related to the slow mode. Under this assumption all the periods in each of the SVAN windows were divided into two groups - the periods lower and higher than 29 days, respectively. In both these groups the period with the maximal amplitude was picked out again in each SVAN window. Consequently, two new sets of periods, each of them comprising 258 new values, were obtained. Within each of both these sets a mean period was calculated and considered to be the period of the given mode at the corresponding latitude. An example of the described determination of two modes of coronal rotation is presented in the upper panel of Fig. 5. Here, analogously to the upper part of Fig. 2, the horizontal lines give the mean periods of rotation of two modes. One may notice that dispersion of the points is lesser for these two sets of points in comparison with that in the upper panel of Fig. 2 drawn for the whole set of data at a given latitude.

As a variant (not presented here) we have performed separation into two modes at all the latitudes but under assumption that, for example, 30 days is a value separating two modes. It was found that the values of the periods with maximal amplitude in each SVAN window and, moreover, their mean values are only slightly sensitive to the choice of the period value separating two modes. In any case, we are justified to insist that the choice of the 30-day separating value enlarges slightly the period of the slow mode and at the higher latitudes that of the fast mode.

In the lower panel of Fig. 5 we demonstrate a possibility to manifest "a mean spectrum" by a sum of two gaussian curves. It is noticeable – in Fig. 5 that the set of points outlining the averaged spectrum apparently splits into two peaks with the maxima at the regions around 27.5 days and 31.0 days. Expression of this set of points by a sum of two gaussian curves gives their maxima namely for those values of periods. Maxima of these gaussian curves approximately correspond to two mean values determined by the method of maximal amplitudes and shown in the upper part of this figure. We note here that a sufficiently hopeful expression of the mean spectrum like the sum of two gaussian curves is possible only in the case of the middle solar latitudes where contribution of both the modes is approximately equal.

The periods of two modes of coronal rotation obtained by the method of maximal amplitudes, with the period of 29 days separating these modes are displayed in dependence on latitude in the upper panel of Fig. 6. The fast mode has period 27 days at low latitudes and is slightly differential – at higher latitudes its period increases up to 28 days. The slow mode displays period of 30.5 days and it is approximately stable.

The results introduced in Fig. 3 and the upper panel of Fig. 6 allow to determine a relative input of the two modes into the total sideral rotation rate of the solar corona. Let the input of the fast mode is D, consequently, the input of the

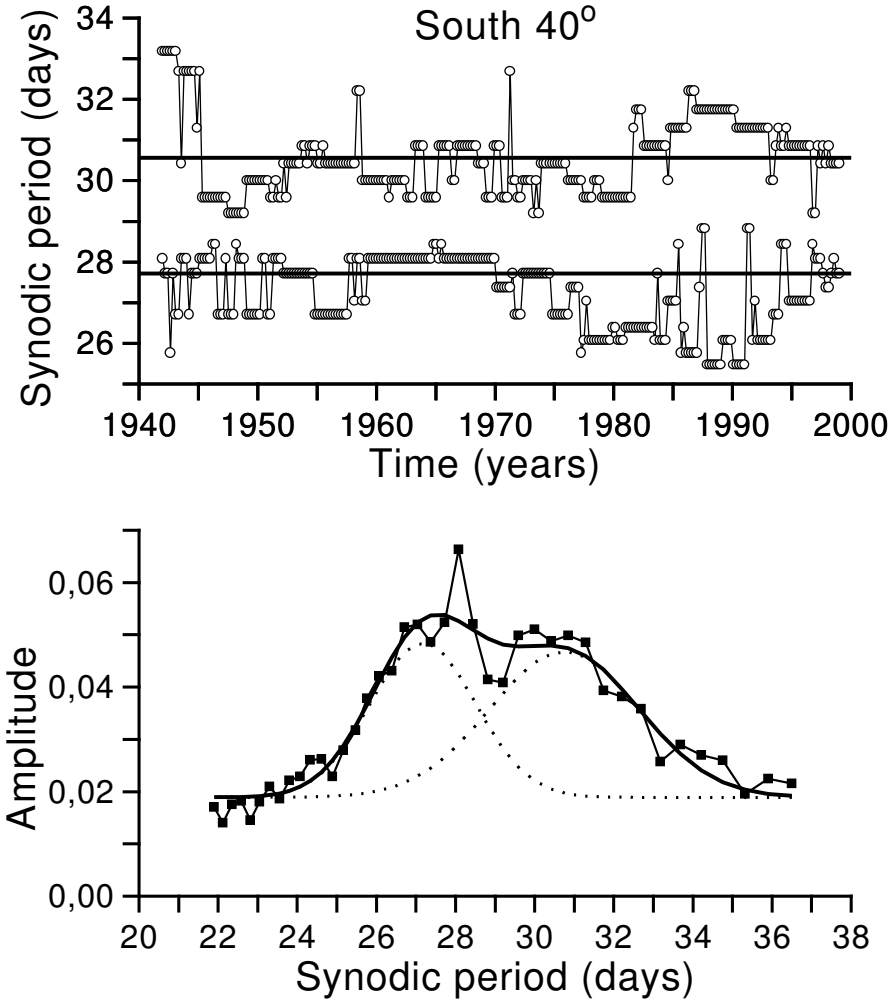

Figure 5. The upper panel represents an example of determination of two modes of coronal rotation for the latitude S 40°. Here, two horizontal lines denote the means of two sets of periods obtained by the procedure as described in the text for the 29-day period separating two modes. The lower panel shows a mean spectrum for the same latitude manifested as the sum of two gaussian curves.

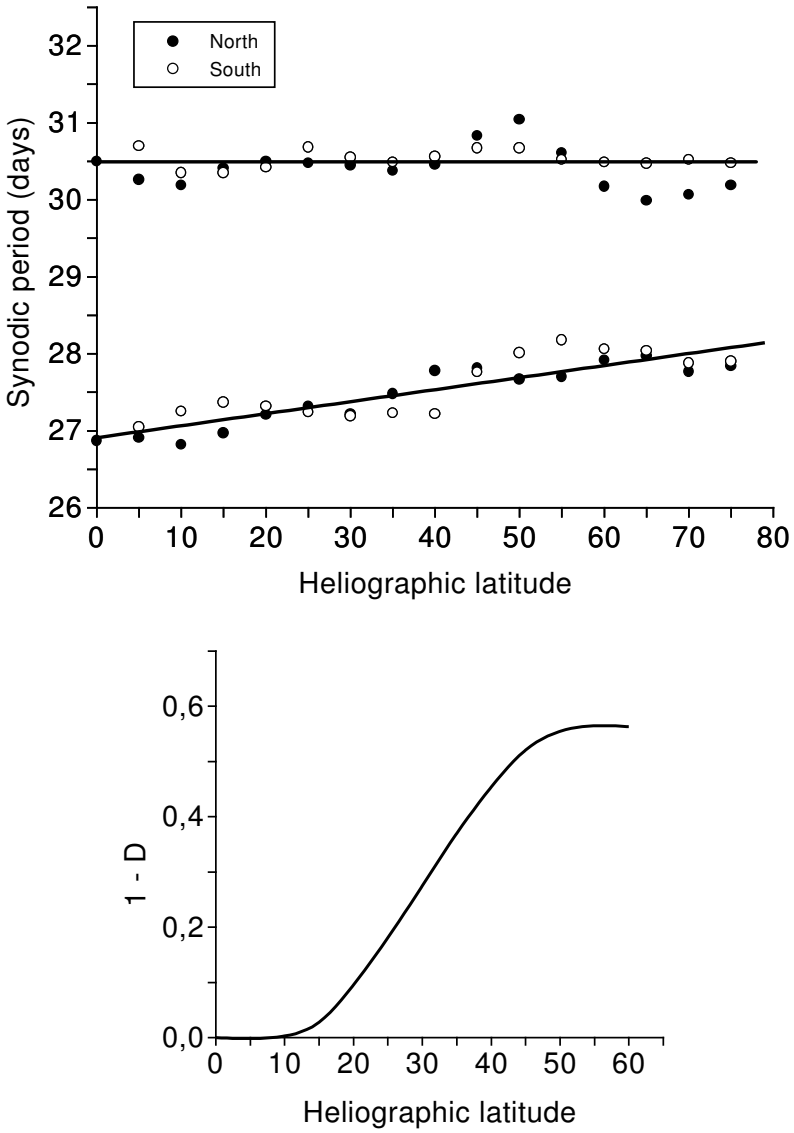

Figure 6. Two modes of coronal rotation in dependence on latitude (upper panel). The open and full circles correspond to the northern and southern hemispheres, respectively. The lower full line represents a mean slightly differential fast mode while the upper horizontal line manifests the latitudinal dependence of a quasi-rigid slow mode. The lower panel demonstrates contribution of the slow mode $1 - D$ to the general summary rotation rate also in dependence on latitude.

slow mode is $1 - D$. The observed angular sideral rotation rate of the corona ω (derived from the upper panel of Fig. 6) can be expressed as

$$\omega = \omega_1 \times D + \omega_2 \times (1 - D), \tag{2}$$

where ω_1 and ω_2 are angular sideral rotation rates of the fast and slow modes, respectively (derived from the lower panel of Fig. 6).

The results of calculations performed by the above formula are presented in the lower panel of Fig. 6. We bring here contribution of the slow mode $1 - D$. Calculations show that at low latitudes, naturally, the coronal rotation completely comes from the fast mode. With an increasing latitude the input of the fast mode successively decreases and, correspondingly, the input of the slow mode increases. Nevertheless, even at high latitudes (see Fig. 6) the input of the slow mode represents about 60% and, therefore, the input of the fast mode still remains relatively high, about 40%. In the first approximation, the percentual input of two modes could be understood as a percentual ratio of the areas occupied by the coronal features rotating faster and slower, correspondingly. In Badalyan et al. (2005) this question is studied in more detail and it is shown that the contribution from both the modes is time-dependent, varying with the solar cycle phase. At the same time, the slow mode becomes relevant at the cycle ascending phase only. In this case, contribution of the slow mode in the averaged general coronal rotation, as presented in the lower panel of Fig. 6 reflects, in fact, temporal variability of this mode.

A possible co-existence of two modes in the rotation of solar features (quasi-rigid and slowly differential rotations) was considered repeatedly in the past: e.g., by Bumba and Howard (1969), Stenflo (1977) for the background magnetic fields; by Ambrož (1973) for calcium flocculi; by Sýkora (1971b), Antonucci and Svalgaard, (1974), Letfus and Sýkora, (1982) for the solar emission corona; and by Mouradian et al. (2002) for radio radiation. The solar rotation represents, in fact, a sum of rotations of different-scale magnetic fields, i.e., it results from the diversity of solar rotation with the latitude and depth in the Sun's body. In this context, the two modes may be identified with the presence and evolution of the local and global magnetic fields on the Sun.

4. Relation to the helioseismic results

In the last years helioseismology has made great progress. Sophisticated experiments allowed, in particular, to describe the rotation rate inside the Sun in dependence on depth and latitude. Summarizing pictures illustrating these achievements were given by, e.g., Kosovichev (2003) and Schou et al. (1998).

Let us make comparison of our coronal rotation rates with the helioseismic results. We have found the synodic period in the equatorial zone (fast mode) to be 27 days. This corresponds to the rotation rate of 13.333 degrees per day. Then, the angular sideral rotation rate is $\omega_1 = 14.319$ degrees per day which

implies the period of rotation 25.14 days representing frequency of 460 nHz. This value well agree with the helioseismic rotation rate (frequency) found for the equatorial surface region and deeper to the tachocline layer. Analogously, our 30.5 days period of rotation (slow mode) corresponds to the angular sideral rotation rate 12.789 degrees per day implying the 28.15 day sideral period of rotation representing frequency 410 nHz. This value corresponds to the helioseismic surface rotation at $45^\circ - 50^\circ$ and/or to the rotation found at the base of the convective zone.

Thus, one may assume that the differential rotation of the solar corona pretty well reflects rotation of the Sun's inner layers. The rotation rate from the solar convective zone emerges to the surface and, at the same time, a mixing of the regions moving with different velocities takes place creating the observed rotation rate of the solar corona. It may be assumed that the active coronal regions situated at low latitudes are governed, to a large extent, by the local magnetic fields the source of which is located at upper part of the under-photospheric layers while, the solar corona of higher latitudes is influenced mostly by the global large-scale fields rooted close to the tachocline layer.

5. Conclusion

Our own data on the Fe XIV 530.3 nm coronal green line brightness, covering almost six solar cycles (1943-2001), have been subjected to the Spectral Variation Analysis (SVAN) to investigate the differential rotation of the solar corona. The following principal results were obtained:

(a) The mean (i.e, averaged over the whole database) synodic period of rotation increases from 27 days at the solar equator to slightly more than 29 days at the latitudes of $\pm 40^\circ$, displaying much slower differentiality than a majority of the solar photospheric phenomena do.

(b) The differentiality of rotation is almost negligible at low latitudes, increases at the latitudes above $\pm 15^\circ$ and disappears at $\pm 40^\circ$. At the higher latitudes the rotation displays practically rigid character with the rotation period of about 29.5 days up to the polar regions.

(c) A number of experimental and theoretical considerations allow to assume that the rotation of the solar corona may be introduced by a superposition of two modes of rotation. The faster one has the period of 27 days and displays slight increase towards the higher latitudes while the slow mode has the period of about 30.5 days. The observed dependence of coronal rotation on the solar latitude apparently results from a combination of the two mentioned modes. A subsequent analysis (Badalyan et al., 2005) has shown that the relative contribution of these two modes into the resulting general rotation of the solar corona is cycle-dependent.

(d) Results of the present study well-agree with the latest achievements of helioseismology. At the same time, the fast and slow modes reflect rotation rates

in the deeper Sun's layers resulting in the corresponding motions of the coronal elements controlled by the local and large-scale solar magnetic fields.

Acknowledgements. This work was partially supported by the Grant 05-02-16080 of the Russian Foundation for Basic Research, by the Grant INTAS 2000-840 and by the VEGA Grant 2/4013/24 of the Slovak Academy of Sciences.

References

Ambrož, P.: 1973, *Bull. Astron. Inst. Czechoslov.* **24**, 80
Antonucci, E., Svalgaard, L.: 1974, *Solar Phys.* **34**, 3
Badalyan, O.G., Sýkora, J.: 2005, *Adv. Space Res.* , submitted
Badalyan, O.G., Obridko, V.N., Sýkora, J.: 2001, *Solar Phys.* **199**, 421
Badalyan, O.G., Obridko, V.N., Sýkora, J.: 2004, *Astron. Astrophys. Trans.* **23**, 555
Badalyan, O.G., Obridko, V.N., Sýkora, J.: 2005, *Astron. Zh.* **82**, 535
Bogart, R.S.: 1987, *Solar Phys.* **110**, 23
Bumba, V., Howard, R.: 1969, *Solar Phys.* **7**, 28
Dzewonski, A., Block, S., Landisman, M.: 1969, *Bull. Seismol. Soc. Am.* **59**, 427
Fisher, R.R., Sime, D.G.: 1984, *Astrophys. J.* **287**, 959
Foukal P.V.: 2004, *Solar Astrophysics (Second, Revised Edition)*, Wiley-VCH Verlag GMBH and Co. KGaA, Weinheim
Gnevyshev, M.N.: 1967, *Solar Phys.* **1**, 107
Gnevyshev, M.N.: 1977, *Solar Phys.* **51**, 175
Hansen, R.T., Hansen, S.F., Loomis, H.G.: 1969, *Solar Phys.* **10**, 135
Howard, R.: 1990, *Solar Phys.* **126**, 299
Kichatinov, L.L.: 2004, *Astron. Zh.* **81**, 176
Kosovichev, A.G.: 2003, in *Proc. of the International Solar Cycle Studies Symposium 2003 "Solar Variability as an Input to the Earth's Environment"*, ed.: A. Wilson, ESA SP-535, Noordwijk, 795
Lanza, A.F., Rodono, M., Pagano, I., Barge, P., Llebaria, A.: 2003, *Astron. Astrophys.* **403**, 1135
Letfus, V., Sýkora, J.: 1982a, *Atlas of the Green Corona Synoptic Charts for the Period 1947-1976*, Veda Publ. House, Bratislava
Letfus, V., Sýkora, J.: 1982b, *Hvar Obs. Bull.* **6**, 117
Libbrecht, K.G., Morrow, C.A.: 1991, in *Solar Interior and Atmosphere*, eds.: A.N. Cox, W.C. Livingston and M.S. Matthews, The University of Arizona Press, Tucson, 479
Mouradian, Z., Bocchia, R., Botton, C.: 2002, *Astron. Astrophys.* **394**, 1103
Newton, H.W., Nunn, M.L.: 1951, *Mon. Not. Roy. Astron. Soc.* **111**, 413
Parker, G.D.: 1986, *Solar Phys.* **104**, 333
Rüdiger, G.: 1989, *Differential Rotation and Stellar Convection (Sun and Solar-type Stars)*, Akademie-Verlag, Berlin
Rybák, J.: 1994, *Solar Phys.* **152**, 161
Rybák, J.: 2001, *Hvar Obs. Bull.* **24**, 135
Schou, J., Antia, H.M., Basu, S., et al.: 1998, *Astrophys. J.* **505**, 390
Schrijver, C.J., Zwaan, C.: 2000, *Solar and Stellar Magnetic Activity, Cambridge Astrophys Series, Vol. 34*, Cambridge Univ. Press, Cambridge

Schröter, E.H.: 1985, *Solar Phys.* **100**, 141
Sheeley, N.R., Jr., Nash, A.G., Wang, Y.-M.: 1987, *Astrophys. J.* **319**, 481
Sime, D.G., Fisher, R.R., Altrock, R.C.: 1989, *Astrophys. J.* **336**, 454
Snodgrass, H.B.: 1992, in *The Solar Cycle*, ed.: K.L. Harvey, Astron. Soc. Pacific Conf. Series, Vol. 27, San Francisco, 205
Stenflo, J.O.: 1977, *Astron. and Astrophys.* **61**, 797
Stenflo, J.O.: 1989, *Astron. Astrophys.* **210**, 403
Stix, M.: 2004, *The Sun (An Introduction), (Corrected Second Edition)*, Springer, Berlin
Storini, M., Sýkora, J.: 1997, *Nuovo Cimento* **20C**, 923
Sýkora, J.: 1971a, *Bull. Astron. Inst. Czechosl.* **22**, 12
Sýkora, J.: 1971b, *Solar Phys.* **18**, 72
Sýkora, J.: 1980, in *Proc. IAU Symp. 91 "Solar and Interplanetary Dynamics"*, eds.: M. Dryer and E. Tandberg-Hanssen, D. Reidel Publ. Co., Dordrecht, 87
Sýkora, J.: 1994, *Adv. Space Res.* **14**, (4)73
Sýkora, J., Rybák, J.: 2005, *Adv. Space Res.* , in press
Trellis, M.: 1957, *Ann. d'Astrophysique* **Suppl. No. 5**,
Waldmeier, M.: 1951, *Die Sonnenkorona 1*, Birkhauser, Basel
Waldmeier, M.: 1971, *Solar Phys.* **20**, 332
Wang, Y.-M., Nash, A.G., Sheeley, N.R., Jr.: 1989, *Science* **245**, 712
Wang, Y.-M., Sheeley, N.R., Jr.: 1993, *Astrophys. J.* **414**, 916